Annals of Forest Science (2017) 74: 54
DOI 10.1007/s13595-017-0654-x

ORIGINAL PAPER

Spatiotemporal analyses of urban vegetation structural attributes using multitemporal Landsat TM data and field measurements

Zhibin Ren [1,2] · Ruiliang Pu [2] · Haifeng Zheng [1] · Dan Zhang [1] · Xingyuan He [1]

Received: 17 June 2016 / Accepted: 20 June 2017 / Published online: 5 July 2017

Abstract

• ***Key message*** **We conducted spatiotemporal analyses of urban vegetation structural attributes using multitemporal Landsat TM data and field measurements. We showed that multitemporal TM data has the potential of rapidly estimating urban vegetation structural attributes including *LAI*, *CC*, and *BA* at an urban landscape level.**

• ***Context*** Urban vegetation structural properties/attributes are closely linked to their ecological functions and thus directly affect urban ecosystem process such as energy, water, and gas exchange. Understanding spatiotemporal dynamics of urban vegetation structures is important for sustaining urban ecosystem service and improving the urban environment.

• ***Aims*** The purposes of this study were to evaluate the potential of estimating urban vegetation structural attributes from multitemporal Landsat TM imagery and to analyze spatiotemporal changes of the urban structural attributes.

• ***Methods*** We first collected three scenes of TM images acquired in 1997, 2004, and 2010 and conducted a field survey to collect urban vegetation structural data (including crown closure (CC), tree height (H), leaf area index (LAI), basal area (BA), stem density (SD), diameter at breast height (DBH), etc.). We then calculated and normalized NDVI maps from the multitemporal TM images. Finally, spatiotemporal urban vegetation structural maps were created using NDVI-based urban vegetation structure predictive models.

• ***Results*** The results show that NDVI can be used as a predictor for some selected urban vegetation structural attributes (i.e., CC, LAI, and BA), but not for the other attributes (i.e., H, SD, and DBH) that are well predicted by NDVI in natural vegetation. The results also indicate that urban vegetation structural attributes (i.e., CC, LAI, and BA) in the study area decreased sharply from 1997 to 2004 but increased slightly from 2004 to 2010. The CC, LAI, and BA class distributions were all skewed toward low values in 1997 and 2004. Moreover, LAI, CC, and BA of urban vegetation all present a decreasing trend from suburban areas to urban central areas.

• ***Conclusion*** The experimental results demonstrate that Landsat TM imagery could provide a fast and cost-effective method to obtain a spatiotemporal 30-m resolution urban vegetation structural dataset (including CC, LAI, and BA).

Handling Editor: Barry Alan Gardiner

Contribution of the co-authors All the co-authors have made contribution to the manuscript. Dr. Haifeng Zheng has collected three scenes of TM images acquired in 1997, 2004 and 2010 and then calculated and normalized NDVI maps from the multitemporal TM images. Dr. Dan Zhang has conducted a field survey to collect urban vegetation structural data (including crown closure (CC), tree height (H), leaf area index (LAI), basal area (BA), stem density (SD), diameter at breast height (DBH), etc.). Dr. Zhibin Ren has designed the general experiment and written the paper. Dr. Ruiliang Pu has helped Dr. Ren write the paper and conducted revision and editing in English for the paper. Dr. Xingyuan He has taken a lot of time to make constructive reviews and advices.

✉ Xingyuan He
hexingyuan@iga.ac.cn

Zhibin Ren
renzhibin1985@163.com

Ruiliang Pu
rpu@usf.edu

Haifeng Zheng
zhenghaifeng@iga.ac.cn

Dan Zhang
zhangdan@iga.ac.cn

[1] Key Laboratory of Wetland Ecology and Environment, Northeast Institute of Geography and Agroecology, Chinese Academy of Sciences, Changchun, Jilin 130102, China

[2] School of Geosciences, University of South Florida, 4202 E. Fowler Ave., NES 107, Tampa, FL 33620, USA

Keywords Spatiotemporal analysis · Urban vegetation structure · Landsat TM imagery · NDVI

1 Introduction

During the last three decades in China, many serious environmental problems have arisen especially in urban areas, which affect human health and sustainability of urban ecosystems (Cao et al. 2009). Urban vegetation is considered as an important component of urban ecosystems contributing a broad array of ecological functions and plays an important role in improving urban environments (McPherson et al. 2005; Dwivedi et al. 2009; Young 2010). Urban vegetation can reduce urban air pollutant concentrations (McPherson and Simpson 1998; Fowler et al. 2004; Nowak et al. 2006), sequestrate atmospheric CO_2 (Nowak and Crane 2002; Myeong et al. 2006; Hutyra et al. 2010), reduce storm water runoff (Xiao et al. 2000; Armson et al. 2013; Kirnbauer et al. 2013), mitigate the urban heat island effect (Shashua-Bar and Hoffman 2000; Bowler et al. 2010), and provide habitats for a variety of organisms (Godefroid and Koedam 2003; Cornelis and Hermy 2004).

Urban vegetation structure (characterized by tree size, crown closure, height, LAI, species composition, etc.) can be considered as a three-dimensional spatial arrangement of vegetation in urban areas (Nowak et al. 1994; Mcpherson et al. 1997). Urban vegetation structural properties/attributes are closely linked to their ecological functions and thus directly affect urban ecosystem process such as energy, water, and gas exchange (Clark et al. 2001; Frolking et al. 2009). Exchanges of evapotranspiration, carbon, and energy that occur in most important ecological processes between urban vegetation ecosystems and the atmosphere strongly depend on urban vegetation structure. Therefore, understanding spatiotemporal dynamic processes of urban vegetation structural attributes is crucial for monitoring, forecasting, and managing urban vegetation at landscape scale for urban planning to improve the urban environment. In addition, accurate and timely estimation of spatiotemporal urban vegetation structural attributes is necessary and useful for urban managers to maximize urban vegetation benefits (urban ecosystem service) and to protect and manage urban environments. Due to rapid urbanization, urban vegetation structure has changed greatly in China (Zhou and Wang 2011), which consequently affects its ecological functions. During the last two decades, there were many studies focusing on the spatiotemporal changes in urban vegetation (Seto et al. 2002; Kong and Nakagoshi 2006; Miller 2012). Most of these studies just focused on the change of urban vegetation cover percentage, which demonstrated that urban vegetation significantly decreased with the continuous increase in urban population and the unprecedented growth of cities. Based on our knowledge, the spatiotemporal dynamics of urban vegetation structure have rarely been studied and thus are not yet fully understood.

As we know, conventional methods for obtaining spatiotemporal information of urban vegetation structure through plot-based sampling measurements are labor-intensive and cost-expensive (Miller and Winer 1984; Lapaixa and Freedman 2010; Trammell, 2011). In addition, these conventional methods usually just provide the estimation of urban vegetation at plot and/or stand levels and it cannot easily be extended to a citywide scale. Consequently, the collection of urban vegetation structural data is only available at very coarse spatial resolution. Also, it is nearly impossible to obtain spatial-temporal maps of urban vegetation structural attributes with a high spatial resolution through the direct field survey method. Lack of spatial-temporal mapping information of urban vegetation structural attributes could diminish our ability to analyze ecological functions of urban vegetation at a landscape level. In order to overcome such limitations of these conventional methods, remote sensing technology has proved to be an important tool for estimating vegetation properties and structure (Frolking et al. 2009) and is considered as a feasible, faster, and repeatable alternative to estimate and map spatially continuous urban vegetation structural attributes over large areas. Given that remote sensing can potentially provide high spatial and temporal resolution data, utilizing remote sensing techniques to study urban vegetation spatiotemporal dynamics can significantly save time and labor compared with the field survey method.

With the increased availability of current and historical remotely sensed data, the remote sensing-based spatiotemporal analyses of vegetation structural attributes with sensitive spectral indices have received increased attention in recent decades because they offer a rapid and cost-effective way to obtain vegetation structure data at a landscape level. Numerous studies have investigated the possibility of using spectral vegetation indices constructed from different remote sensing data to estimate vegetation structure (e.g., Franklin and Hiernaux 1991; Roy et al. 1991; Cohen et al. 1995; Kayitakire et al. 2006). However, although the application of high-resolution remote sensing sensors such as QuickBird and IKONOS are receiving increasing attention, moderate-resolution imagery such as Landsat TM sensor is still a preferred data source. Landsat TM (or ETM+ or OLI) imagery is widely used and is easily accessed over all the world for extracting and estimating vegetation structural attributes. The most commonly used spectral indicator extracted from TM or ETM+ or OLI imagery is the Normalized Difference Vegetation Index (NDVI) based on the red band and near-infrared band. Many researchers have demonstrated that the NDVI is significantly correlated with ground measured vegetation structural attributes such as crown closure, stem density, diameter at breast height, tree height, basal area, leaf area index, biomass, etc. (Turner et al. 1999; Ingram et al. 2005;

Freitas et al. 2005; Ji et al. 2012). Although previous studies have achieved some degree of success in estimating vegetation structural attributes from Landsat sensors' data in natural vegetations worldwide, their conclusions in terms of relationships between vegetation structural attributes and NDVI vary, depending on the characteristics of the study areas (Lu et al. 2004). Urban vegetation is usually heterogeneous, fragmented, and scattered and surrounded by many impervious surfaces and is very different from natural vegetations. Therefore, the relationships found between NDVI and natural vegetation structural attributes might be different from those between NDVI and urban vegetation structural attributes. Whether NDVI extracted from Landsat imagery can still be used for estimating urban vegetation structural attributes remains unknown. Based on our literature review, existing studies mostly focused on monitoring urban land cover change including vegetation canopy cover change using Landsat data (Rogan et al. 2003; Du et al. 2010; Schneider 2012), but there are few studies on estimating urban vegetation structural attributes with TM or ETM+ imagery. Therefore, further research on the potential of using TM imagery for extracting and estimating urban vegetation structural attributes is necessary.

Using field observations and Landsat TM images data acquired in three different years (1997, 2004, and 2010) from the city of Changchun, China, this study aims at developing a faster and cost-effective method to obtain spatiotemporal urban vegetation structure information at 30-m resolution. The substantive research objectives include (1) examining the usefulness of TM image data acquired at different times in estimating spatiotemporal urban vegetation structural attributes, (2) developing algorithms for estimating urban vegetation structural attributes by coupling field measurements with the TM data, (3) producing spatiotemporal maps of urban vegetation structural attributes at a 30-m resolution, and (4) exploring the spatial patterns and analyzing dynamics of urban vegetation structural attributes over the study area in the city of Changchun, China, from 1997 to 2010.

2 Methods

2.1 Study area

This study was conducted in the central city of Changchun (125°09′–125°48′E, 43°46′–43°58′N) (Fig. 1), which is the capital of Jilin province and an important social-economic center of northeastern China. The city of Changchun is located in the hinterland of the Northeast Plain with a total population of 3.6 million by the end of 2010. The urban central area in Changchun City covers approximately 284.7 km^2. This region is characterized by a continental climate of the North Temperate Zone with the obvious variation of four seasons. The average total yearly rainfall is 567 mm. The average temperatures of cold winter and hot summer in the region are −14 and 24 °C, respectively. Changchun is called a "forest city" with a vegetation coverage of 45% and has a very abundant vegetation resource with 43 families, 86 genus, and 211 species (Zhang et al. 2015). The four major species are Poplar (*Populus hopeiensis*), Willow (*Salix babylonica*), Elm (*Ulmus pumila*), and Chinese pine (*Pinus thunbergii*). In addition, Changchun has experienced an accelerated process of urbanization since 1979. Increases in the urban population and urban built area have accelerated in recent decades (Huang et al. 2009), which may have resulted in changes of urban vegetation structure and species composition. Changchun is, thus, an interesting area for exploring the potential of using multitemporal TM data to analyze spatiotemporal dynamics of urban vegetation structural attributes.

2.2 Image data and processing

The three scenes of TM images with a spatial resolution of 30 m were acquired on June 14, 1997, June 01, 2004, and September 22, 2010 with a cloud cover less than 5%, in order to calculate NDVI index maps. The atmospheric correction for the TM images was first undertaken by using the dark-pixel subtraction method (Franklin and Giles 1995). Then the TM raw digital numbers (DN) were converted into surface radiance values by using gain and offset coefficients following the procedures provided by Chander and Markham (2003) prior to the calculation of NDVI in ENVI 4.6 (ITT Visual Information Solutions, Boulder, USA). Next, the TM images were geo-referenced to UTM coordinate system with a root mean square error (RMSE) of less than 0.5 pixel (15 m) by using 33 ground control points taken from topographic maps. The TM images were resampled into a pixel size of 30 m × 30 m by the cubic convolution method during the image rectification. The NDVI index was then calculated from the TM images in ENVI 4.6 through NDVI = (b4 − b3)/(b4 + b3), where b3 and b4 are surface radiance values in TM bands 3 and 4, respectively. To conduct spatiotemporal dynamic analyses of urban vegetation structural attributes with the multitemporal TM images, it is necessary to normalize NDVI maps calculated from the multitemporal TM images (1997, 2004, and 2010) to eliminate changes of light conditions caused radiometric variation of the three scenes of TM images. In this study, a modified relative correction method, which is the pseudo-invariant features (PIF) method (Schott et al.1988) and improved by selecting PIFs manually for different imagery (Yang and Lo 2000), was adopted. This modified method improves statistical consistency by using the same selected regions for all images. In our study, 45 spatial evenly distributed regions of interest for invariant features (including 15 from roads, 20 from roof tops, and 10 from water bodies) located on the multitemporal images were manually selected. The average NDVI in each interest region was

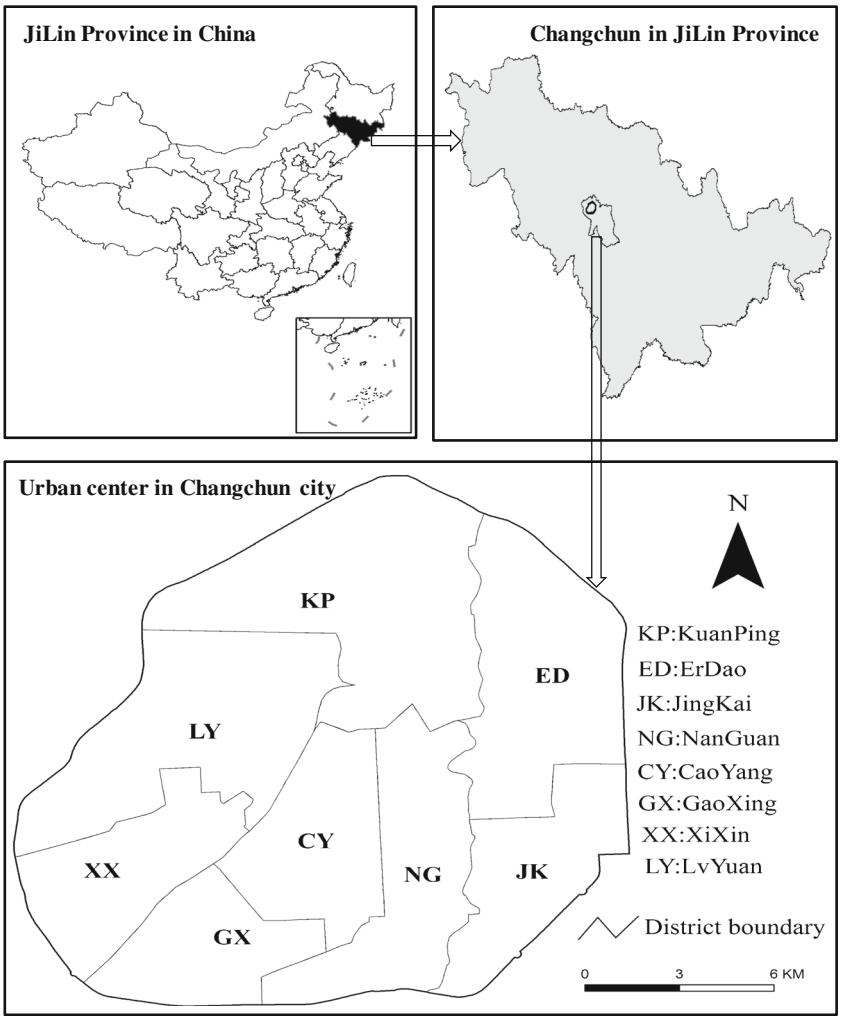

Fig. 1 The study area located within the fourth-loop road in the city of Changchun, China

then used to develop a linear normalization model between the reference image (2010) and the subject (i.e., uncorrected) images (1997 and 2004). Normalized subject images (Fig. 2) were produced using the following equation:

$$NDVI_{\mathrm{ref}} = aNDVI_{\mathrm{sub}} + b$$

where $NDVI_{ref}$ is the reference image (i.e., 2010 image), and $NDVI_{sub}$ is the subject images (i.e., 1997 and 2004 images). The scene normalization coefficients and image statistics of NDVI before and after normalization are listed in Tables 1 and 2.

2.3 Sampling design and field measurements

In this study, 69 random plots (sampling plots) throughout the study area were established for collecting field measurements of urban vegetation structural attributes. We set the 69 plots by using the method used in the UFORE Model (Nowak et al. 2003) during July and August, 2011 and 2012 (Fig. 3). Urban vegetation in our plot survey area is mostly dominated by mature trees, and thus, there was no significant change of urban forest structural attributes during the 1- or 2-year difference (compared to the 2010 image). Therefore, the time difference between imaging time (2010) and field survey (2011) can be ignored. The sampling plots were randomly deployed by the method in the UFORE Model by the aid of the ArcGIS tool (Environmental Systems Research Institute, Redlands, USA) to ensure representative to the major landcover types such as residential areas, road areas, park areas, and commercial areas appearing in the city of Changchun. Moreover, a sampling plot was required to be located in a relatively homogenous patch greater than 1600 m^2. In this study, each of the 69 sampling plots was defined as a 30 × 30 m^2 (0.09 ha) to represent a TM pixel size. The coordinates of each sampling plot were recorded by using a high-accuracy global positioning system (MG838GPS, UniStrong company, Beijing, China) with an accuracy of better than 1 m, which were used to extract NDVI values from multitemporal TM-derived NDVI maps later on. A total of 2097 individual trees were

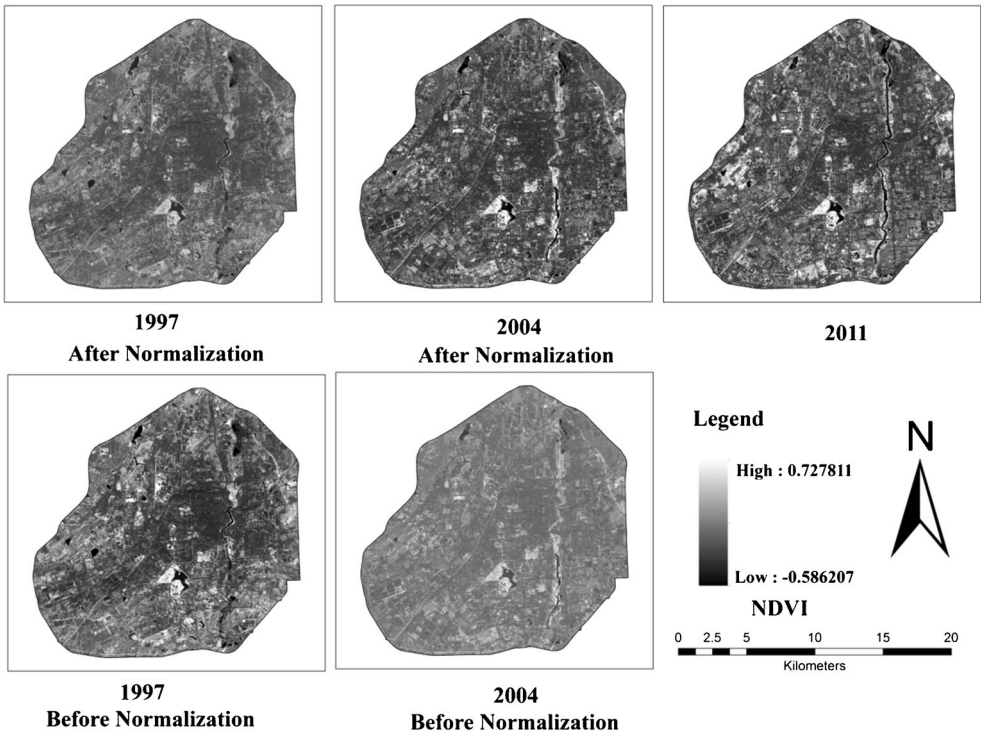

Fig. 2 The NDVI images before and after normalization

measured from the 69 sampling plots. At each sampling plot, all urban vegetation structural attributes including tree species, vegetation types such as conifers and broad-leaves, stem density (SD), diameter at breast height (DBH), tree height (H), leaf area index (LAI), crown closure (CC), and basal area (BA) were measured and recorded.

The SD was defined as number of trees (N) per unit area (n/ha) (Eq. 1). The DBH of each tree within a plot was measured directly using an optical instrument (RD100, Laser Technology Inc., Centennial, USA) and then an average of DBH value was calculated by averaging all sampled trees in the plot (cm) (Eq. 2). The H of each tree within a plot was also measured directly by an optical instrument (RD1000, Laser Technology, Inc., Centennial, USA), and then an average of H value was calculated by averaging all sampled trees in the plot (cm) (Eq. 3). The BA index was defined as a ratio of the total cross-sectional area of all trees per unit area (m^2/ha). It was calculated from the DBH value in a plot using Eq. 4. The CC was measured with a fish-eye camera (AF DX Fisheye, Nikon Corporation, Tokyo, Janpan) with a total accuracy of ±3%, which is defined as a ratio of the fractional area (projected vertically) of tree canopy in a sampling plot to the plot area. The LAI was directly measured with a TRAC (Tracing Radiation and Architecture of Canopies, 3rd Wave Engineering, Nepean, Canada) with a total accuracy of ±0.05, which is defined as a ratio of all one-side leaf area in a sampling plot to the plot area in this study.

$$SD(\mathrm{n/ha}) = \mathrm{N}/0.09 \tag{1}$$

$$\mathrm{DBH(cm)} = \frac{\sum_{i}^{N} \mathrm{DBH}_i}{N} \tag{2}$$

$$H(\mathrm{m}) = \frac{\sum_{i}^{N} H_i}{N} \tag{3}$$

$$\mathrm{BA}\left(\mathrm{m^2/ha}\right) = \frac{\left[\sum_{i}^{N} \pi(\mathrm{DBH}_i/2)^2\right]}{0.09} \tag{4}$$

Where N is the number of trees in a sampling plot for all equations. After the field measurements were conducted, NDVI values were extracted from the normalized NDVI images in ArcGIS 9.3 with the coordinates of each sampling plot for later statistical analyses.

Table 1 The image normalization coefficients and the correction coefficients for each subject image

	1997	2004
a	1.109	0.855
b	0.015	−0.003
R^2	0.904	0.853

Table 2 NDVI statistics before and after normalization

		Max	Min	Mean	StD
1997	Before	0.54	−0.39	0.07	0.09
	After	0.61	−0.42	0.09	0.11
2004	Before	0.72	−0.59	0.08	0.12
	After	0.62	−0.49	0.07	0.11
2010		0.64	−0.43	0.09	0.13

Fig. 3 Map of 69 sampling plots in the city of Changchun

2.4 Regression modeling analyses and mapping of urban vegetation structural attributes with NDVI maps

In order to explore relationships between NDVI and urban vegetation structural attributes for estimating urban vegetation structural attributes, correlation analyses between the measurements of the set of urban vegetation structural attributes collected from the 69 plots and corresponding NDVI values extracted from the 2010 NDVI map were first conducted. Then the corresponding regression models between NDVI and urban vegetation structural attributes were also established to uncover quantitative relationships between them. In these analyses, the NDVI was used as an independent variable while urban vegetation structural attributes were used as dependent variables. In this study, coefficients of determination (R^2) for regression analyses between NDVI and urban vegetation structural attributes were calculated to assess the relationships. All statistical analyses were carried out with the standard statistical software, SPSS (Version 19.0) (IBM Corporation, New York, USA).

In this study, the 2010 urban vegetation structural attribute maps were created by calculating pixel-based urban vegetation structural attribute values using the regression models developed with NDVIs extracted from 2010 NDVI image at the 69 plots and 2012–2013 field survey data. We also created spatio-temporal urban vegetation structural attribute maps from normalized NDVI images calculated from 1997 and 2004 TM images using the regression models of urban vegetation structural attributes, developed with the 2010 NDVI image. Based on these pixel-based multi-year maps of urban vegetation structural attributes, the number of pixels with vegetation cover greater than 0% was also calculated for the three different years.

3 Results

3.1 Regression models for estimating urban vegetation structural attributes

Table 3 lists descriptive statistics for NDVI and urban vegetation structural attributes. From the table, we can easily see that

Table 3 Descriptive statistics of urban vegetation structural attributes and NDVI calculated with all sampling plots (n = 69)

Urban vegetation structure and NDVI	Max	Min	Mean	StD
Stem density (SD, n/ha)	594	99	277.2	97.4
Diameter (DBH, cm)	31.5	7.5	17.5	5.7
Height (H, m)	19.5	3.4	8.8	3.3
Leaf area index (LAI)	13.79	0.4	5.33	3.2
Crown closure (CC, %)	96.8	2.1	50.2	23.7
Basal area(BA, m^2/ha)	30.3	0.3	9.1	5.4
NDVI (year 2010)	0.64	0.06	0.3	0.2

the urban vegetation index, NDVI, had a relatively large range with a mean value of 0.3 and a standard deviation of 0.2. It is also clear in the table that all the urban vegetation structural attributes (SD, DBH, H, LAI, CC, and BA) also varied greatly among the sampling plots in terms of their corresponding mean values and corresponding standard deviations. Table 4 presents the Pearson's correlation coefficients between NDVI and urban vegetation structural attributes. In this table, the correlation analysis results show that leaf area index (LAI), crown closure (CC), and basal area (BA) were all significantly related to NDVI, whereas stem density (SD), diameter at breast height (DBH), and tree height (H) were not. Compared to the correlation analysis results derived from natural vegetations (e.g., Ingram et al. 2005; Freitas et al. 2005; Ji et al. 2012), this suggests that NDVI could be used as a good predictor of some of urban vegetation structural attributes to build urban vegetation structure prediction models.

In order to produce the spatiotemporal maps of urban vegetation structural attributes from historical TM imagery (thus historical NDVI maps), it is necessary to develop the regression models between NDVI and urban vegetation structural attributes. As a result in this study, the three regression models have been established between NDVI and three urban vegetation structural attributes (i.e., LAI, CC, and BA) (Fig. 4). In Fig. 4, it is clear that the CC had a positive linear relationship with NDVI. When NDVI increased 0.1, the CC increased approximately 14%. The linear regression model derived from the 69 plot data with NDVI as independent variables could account for 84% of the total *CC* variance. However, Fig. 4 shows that the LAI and BA attributes had positive non-linear relationships with NDVI. The non-linear models with NDVI as independent variables could explain 58 and 63% of total LAI and BA variance, respectively. Finally, the established regression models were applied to produce maps of CC, BA, and LAI from normalized historical NDVI images of 1997, 2004, and 2010, respectively.

3.2 Spatiotemporal analysis of urban vegetation structural change

With the regression models from Fig. 4, the urban vegetation structural attribute maps for years 1997, 2004, and 2010 were created (Fig. 5). By analyzing these pixel-based multi-year maps of urban vegetation structural attributes in a GIS format, we found that urban vegetation structure was highly dynamic between the years 1997, 2004, and 2010 (Fig. 5). The number of pixels with vegetation decreased gradually from 1997, 2004, to 2010 (Table 5 and Fig. 5). Percentage cover of urban vegetation canopy (i.e., CC%) was 20.52, 14.29, and 16.65% of the entire study area in 1997, 2004, and 2010, respectively (Table 5). Urban vegetation crown closure in this study area in the city of Changchun significantly decreased by 6.23% from 1997 to 2004, but slightly increased by 3.36% from 2004 to 2010 (Table 4). The net change from 1997 to 2010 decreased 3.87% or 11.02 km^2. Leaf area index (LAI) in the study area (i.e., average LAI) was 0.76, 0.51, and 0.61 in the years 1997, 2004, and 2010, respectively (Table 5). Urban vegetation LAI decreased by 0.25 from 1997 to 2004, but increased by 0.10 from 2004 to 2010 and the net change from 1997 to 2010 was a decrease of 0.15. The average BA of urban vegetation in the study area (i.e., total basal area (m^2)/study area (ha)) was 2.28, 1.69, and 2.04 m^2/ha in the years 1997, 2004, and 2010, respectively (Table 5). Urban vegetation BA decreased by 25.88% from 1997 to 2004, but increased by 20.7% from 2004 to 2010. The net decrease for basal area from 1997 to 2010 was 10.53%.

Figure 5 shows that estimated values of urban vegetation CC, BA, and LAI decreased from 1997 to 2004 and increased sharply from 1997 to 2010 (Fig. 5) by making statistical analysis of pixel values with urban vegetation structural attributes in the study area. Figure 6 demonstrates the frequency distribution of CC, BA, and LAI for urban vegetation. The CC, BA, and LAI class distributions were all skewed toward low values. The results in Fig. 6 show that the CC with the highest frequency was 20–40%. The frequency of CC from 0 to 40% was 81, 87, and 68% in 1997, 2004, and 2010, respectively. The frequency of lower CC (0–40%) increased from 1997 to 2004, but decreased from 2004 to 2010. The values in the LAI map were clustered in the range from 0 to 1.5. The frequency of lower LAI (0–1.5) increased from 82% in 1997 to 90% in 2004, but decreased from 90% in 2004 to 38% in 2010. About 6.85% of LAI values were above 6 in 2010, but there are very few pixels with $LAI > 6$ in 1997 and 2010. The BA index with the highest frequency was in the range 0–2.5 m^2/ha. The frequency of *BA* from 0 to 2.5 m^2/ha was 38, 56, and 27% in 1997, 2004, and 2010, respectively. However, the frequency of higher *BA* index (>2.5 m^2/ha) decreased from 1997 to 2004, but increased from 2004 to 2010.

In 1997, most of urban vegetation was distributed in suburban areas (Fig. 5). With the urban expansion, an obvious

Table 4 Pearson's correlation coefficients between NDVI and urban vegetation structural attributes ($n = 69$)

	Stem density (n/ha)	DBH (cm)	Height (m)	Basal area (m^2/ha)	Leaf area index	Crown closure (%)
NDVI	0.086	0.127	0.171*	0.806*	0.711**	0.914**

*Correlation is significant at $\alpha = 0.05$ level (two-tailed);

**correlation is significant at $\alpha = 0.01$ level (two-tailed)

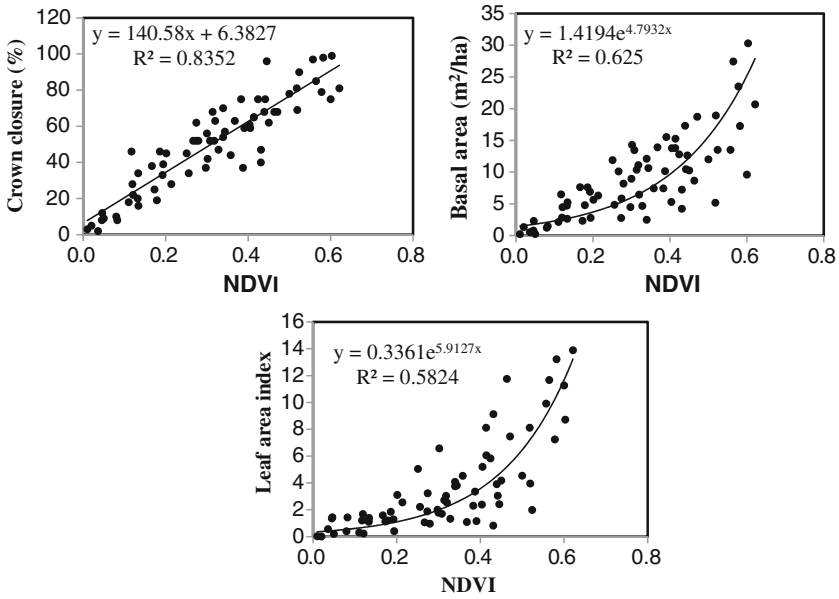

Fig. 4 Regression analyses of NDVI with urban vegetation structural attributes: CC, LAI, and BA (n = 69)

urban vegetation loss first occurred in the urban fringe and suburban area and the CC, BA, and LAI of the urban vegetation changed greatly. Figure 7 demonstrates spatiotemporal changing patterns of mapped urban vegetation structural attributes over the study area. The results in Fig. 7 show that the greatest changes of CC, BA, and LAI occurred in the suburban area. From 1997 to 2004, CC, BA, and LAI of urban vegetation decreased a lot in suburban areas, but there was still a slight increase of CC, BA, and LAI in urban central areas. From 2004 to 2010, the CC, BA, and LAI values across our study area generally increased, especially in suburban areas. However, there was still overall a decrease of CC, BA, and LAI in our study area from 1997 to 2010. In addition, Fig. 5 illustrates that CC, BA, and LAI of urban vegetation showed a trend of decreasing from suburban areas to central business district (CBD) areas in the city of Changchun for the years 1997, 2004, and 2010. Moreover, CC, BA, and LAI of urban vegetation on road sides, industrial areas, and residential areas usually had relatively low values. In urban park areas, their values were fairly high, especially in 2010.

4 Discussion

4.1 Theoretical implications

The spatiotemporal analysis of urban vegetation structural attributes from the remotely sensed imagery is very important for trying to understand the dynamics of urban vegetation structural attributes and to provide information for planning and management of urban vegetation to maximize its functions. The results from this study show that not all the selected urban vegetation structural attributes could be estimated by using NDVI extracted from multitemporal TM imagery. The Landsat remote sensing technique did not work well for the estimation of stem density (SD), mean DBH, and height (H) of urban vegetation, although these three attributes can be well estimated by NDVI in natural vegetations (e.g., Lu et al. 2004; Ingram et al. 2005; Freitas et al. 2005; Hall et al. 2006). One possible reason might be that the environment of urban vegetation is very different from that of natural vegetations. Not only does it contains vegetation but also other features such as buildings, roads, and other impervious areas that can influence pixel-based spectral response and create many mixed pixels. Therefore, the mixed pixel issue might be the main reason for confusion in estimating urban vegetation structural attributes. In addition, the mixed pixel effect may behave differently for different urban vegetation structural attributes. The SD, H, and DBH for urban vegetation may be more influenced by the mixed pixel effect in the city area than other urban vegetation structural attributes. Moreover, it is believed that SD, H, and DBH for both urban and natural vegetations are more difficult to measure by remote sensing than other properties of vegetation characteristics (Freitas et al. 2005; Hall et al. 2006). However, some vegetation structural attributes, such as crown closure (CC), basal area (BA), and leaf area index (LAI) could be still predicted by NDVI in this study. This might be because they were more correlated to an "area" property of vegetation characteristics, which is more easily sensed by a remote sensing sensor than other properties of vegetation characteristics (Pu and Gong 2004). In addition, due to there being more mixed pixel along roads and other impervious areas than in urban parks, it may be more difficult to estimate urban vegetation structural attributes by remote sensing in urban roads and impervious areas than in urban parks.

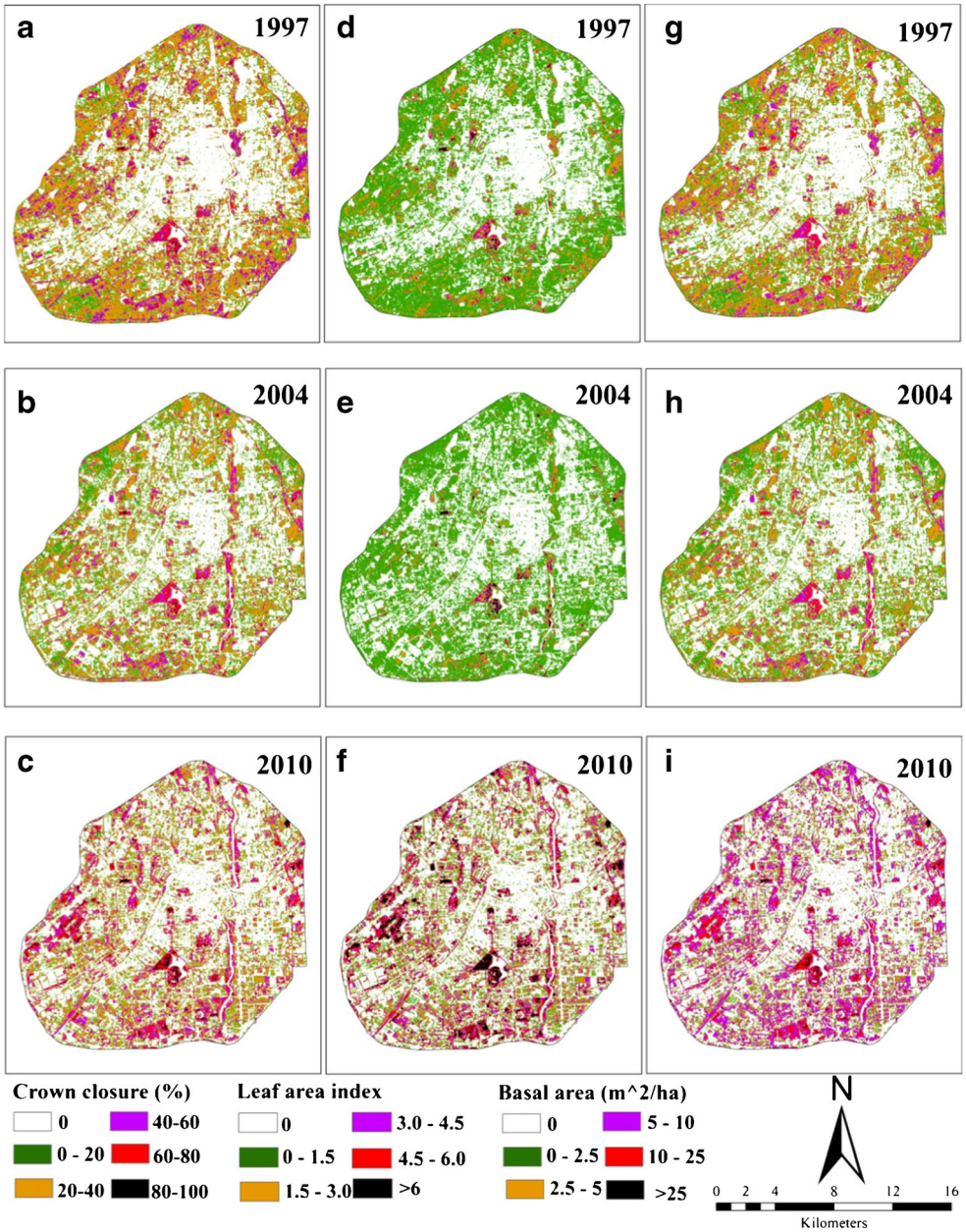

Fig. 5 Spatiotemporal distribution of mapped urban vegetation structural attributes across the study area in the city of Changchun (CC: **a**, **b**, **c**; LAI: **d**, **e**, **f**; BA: **g**, **h**, **i**)

The major limitation of using vegetation indices (VIs) to estimate vegetation structural attributes is that VIs frequently lose sensitivity and saturate at moderately high basal area (BA) and leaf area index (LAI). Many studies (e.g., Baret and Guyot 1991; Gower et al. 1999; Gray and Song 2012) have reported that models between VIs and LAI or BA are

Table 5 Summary of some urban vegetation attributes within the study area in the city of Changchun, China

Imaging year	Vegetated pixel percentage (%)	Canopy cover (%)	Leaf area index	Basal area index (m^2/ha)
1997	60.57	20.52	0.76	2.28
2004	55.06	14.29	0.50	1.69
2010	47.65	16.65	0.61	2.04

Vegetated pixel (pixels with >0% vegetation cover) percentage (%) = pixels with vegetation cover/all pixels in study area; canopy cover (%) = urban vegetation crown area/ study area; Leaf area index = one-side leaf area/ study area; Basal area index = total basal area/study area.

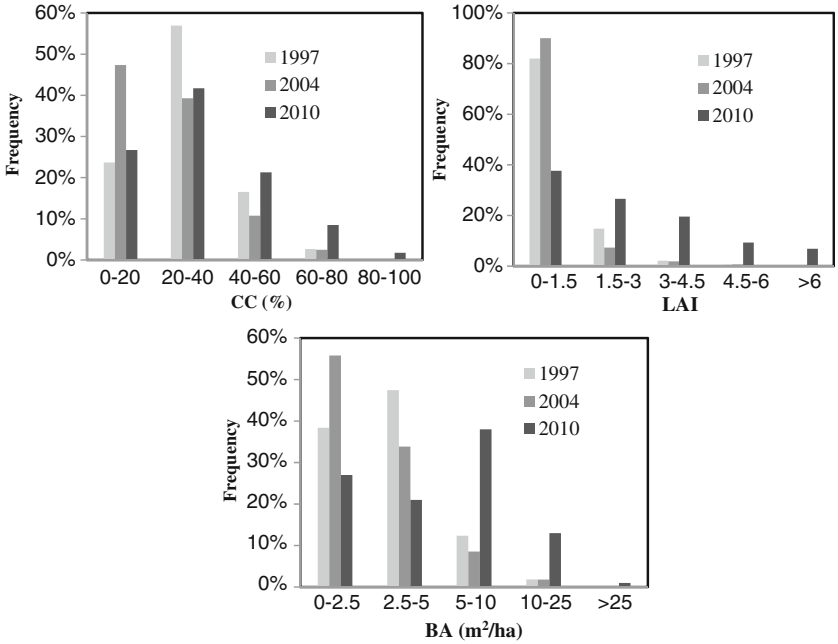

Fig. 6 Histograms of the frequency statistics for urban vegetation structural attributes: CC, LAI, and BA, calculated from pixels with vegetation cover > 0% in the study area of Changchun, China

curvilinear, and there is a trend of saturation in the VIs. For example, Franklin (1986) investigated the relationship between spectral VIs derived from satellite data and field measured BA data and found that as the BA increases, there is a trend of saturation in a VI. The non-linear equations between NDVI and either BA or LAI found in this study for estimating the two urban vegetation structural attributes using TM data showed this limitation. Our results show that the saturation effect of the NDVI still exists in the urban environment similarly to natural vegetation. However, such a limitation could be mostly ignored since LAI and BA from most urban vegetated areas in this study were less than 6–7 and 25–30 m^2/ha (Fig. 4), respectively.

In addition, our experimental results for estimating urban forest structural attributes using TM images also imply that the optical sensors such as Landsat TM can mainly detect the upper crown surface of forests in two-dimensional space and it remains a challenge for optical sensors to extract vertical structural information for urban forests such as tree height, which can influence the estimation of the three-dimensional structures of urban forests. LiDAR imagery can provide accurate measurements of urban forest structures in a vertical plane. It measures the vertical distance and provides tree height and canopy height information, thus potentially enabling improved the accuracy of estimating three-dimensional structures of urban forests such as LAI (Lefsky et al. 1999; Weishampel et al. 2000; Naesset and Okland 2002). Therefore, the multi-sensor approaches that integrate optical remote sensing data with LiDAR imagery data should be used to characterize urban forest structures in future research (Figueiredo et al. 2016).

4.2 Management implications

Using multitemporal satellite images potentially enables mapping of urban vegetation structure regionally and historically. Our results suggest that some spatiotemporal urban vegetation structural attributes (e.g., LAI, CC, and BA) could be estimated from multitemporal TM data. Our results also demonstrate the potential of using the multitemporal TM imagery to map past urban vegetation structural attributes.

The urban vegetation structural attribute maps produced from TM images have important implications for urban planners to maximize the ecological benefit of urban vegetation, particularly for cities where urban vegetation is still being established. In this study, we found that urban vegetation in the well-urbanized region of the city of Changchun was very dynamic, and the number of vegetated pixels decreased gradually from 1997 to 2004 and from 2004 to 2010 (Table 5 and Fig. 5). The changes in urban vegetation in the study area from 1997 to 2010 could be a response to the urbanization and greening policies of the city government (National Bureau of Statistics of China, 1985–2014). The decrease of urban vegetation might be also because the city of Changchun has experienced rapid urbanization since 2000. Changes in the number of vegetated pixels in the study area as well as urban vegetation spatial patterns may have significant impacts on its function in urbanized areas. For example, the net decrease in the number of vegetated pixels, mostly converted to impervious surfaces, would significantly affect the formation of urban heat islands in the city of Changchun. However, in this study, we found that the urban vegetation structural attributes (i.e., CC, LAI, and BA) in the study areas lightly

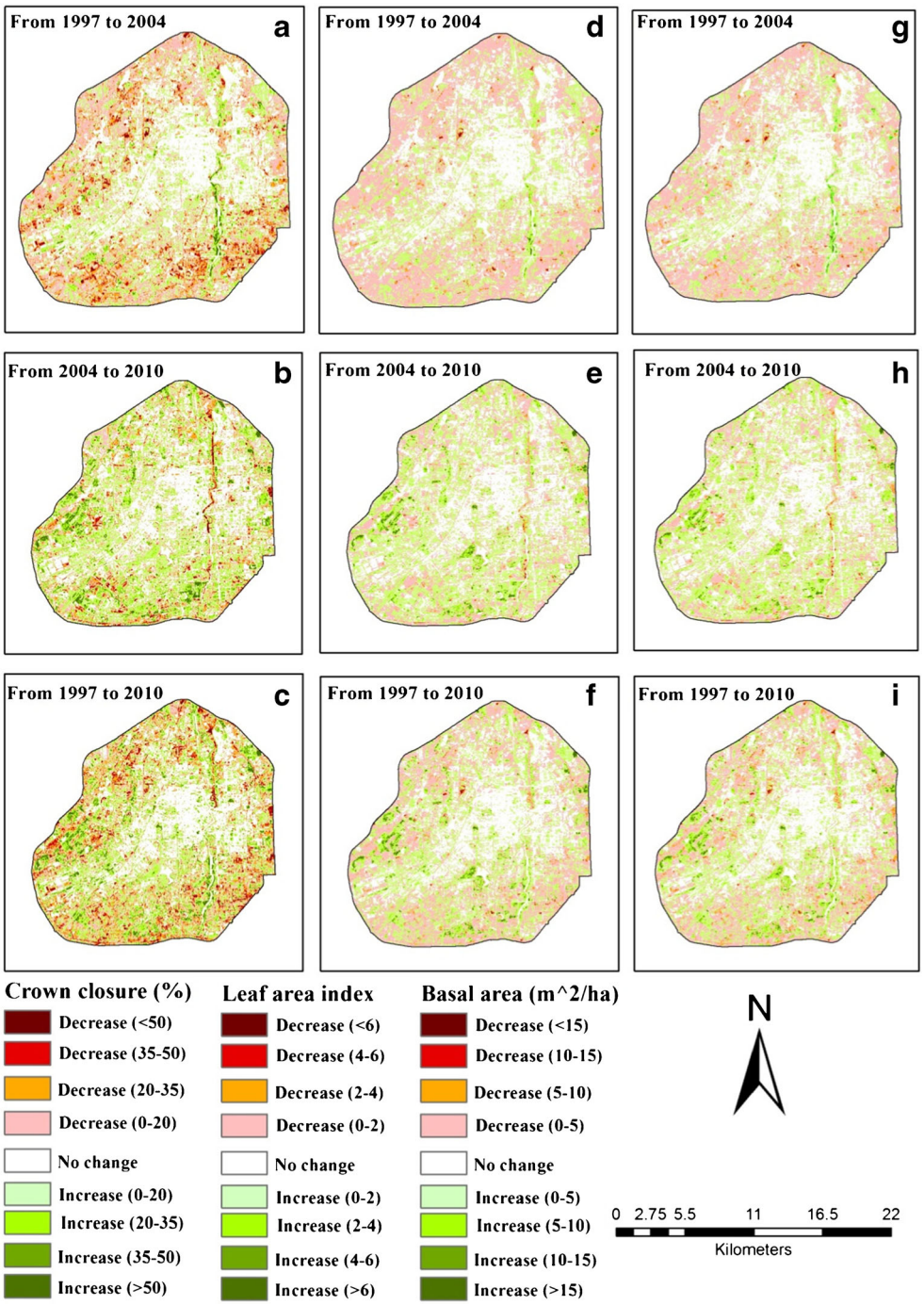

Fig. 7 Spatiotemporal changing patterns of mapped urban vegetation structural attributes over the study area in the city of Changchun (CC: **a**, **b**, **c**; LAI: **d**, **e**, **f**; BA: **g**, **h**, **i**)

increased from 2004 to 2010. This phenomenon may be explained by the following two points: (1) It could be caused by growth of the vegetation. Since 2005, the local governments in Changchun have paid more attention to the management of urban vegetation, which could enhance the rapid growth of trees. (2) This might be also due to the efforts to increase urban vegetation quality and quantity and establishing more urban forest parks by the local governments. With a rapid urbanization in Changchun since 1990, much urban vegetation has been destroyed and become more scattered, which resulted in many serious environmental problems affecting human health. Having realized the important role of urban vegetation in urban ecosystems, local governments in China have set out a series of policies and invested a large amount of money to introduce green elements into urban areas in order to improve urban environment. Among them are establishing more new urban forest parks and community gardens, planting more trees along roads, and especially paying more attention to management of existing urban vegetation

in recent 10 years. From our results, we see that the various greening policies introduced by the city government appear to have contributed to the increase of the average urban vegetation structural attributes of CC, LAI, and BA in the last decade. However, our results also show that most areas in the study area are still covered by vegetation with low CC, BA, and LAI values, which could limit their ability to provide ecological benefits. Therefore, some measures still need to be taken further by urban managers to increase CC, BA, and LAI. Some suggested measures might include designing trees, shrubs, and grass in an optimal way such as selecting the most appropriate tree species, and pruning and shaping canopies. In practice, the multilayer forest communities with high CC and LAI are obviously the most effective in terms of the ecological effect (Ren et al. 2013). In addition, our results from this study also show that urban vegetation cover in suburban areas was higher than that in CBD areas. It suggests that urban vegetation was unevenly distributed within a city area, which could lead to the environmental inequity (Landry and Chakraborty 2009; Tooke et al. 2010). Therefore, urban planners and policy makers should be concerned with the distribution of urban vegetation and plant more trees to distribute vegetation more evenly.

Our results suggest that the NDVI derived models could be used to estimate some urban vegetation structural attributes over the city areas from TM imagery. However, there are still some drivers of uncertainty for urban vegetation structural prediction models (Convertino et al. 2014). It should be noted that the NDVI is easily affected by phenology and season (Townshend and Justice 1986; Piao et al. 2003; Guo et al. 2007), which may result in change of relations between vegetation index and urban vegetation structures with the time of year. In our study, TM images with a resolution of 30 m × 30 m and sampling plots with a size of 30 m × 30 m were used to uncover the relationships between vegetation index and urban vegetation structural attributes. However, the relationships between them may change across different scales (Li et al. 2013; Harold et al. 2014). More research is needed on the effect of plot size and image resolution on the relationship between urban forest structure and vegetation indices. Some studies found that the vegetation indices such as NDVI change across different climatic conditions and cities (Marc et al. 2010; Martin et al. 2014). Therefore, such a change of the vegetation indices derived from different geographical areas may result in different relationships between the vegetation indices and urban forest structural attributes. In addition, the different climatic conditions, specifically precipitation and temperature, as well as the individual characteristics (e.g., city size, building density and height, dominant vegetation age, etc.) of a city may also significantly influence relationships between NDVI and urban vegetation structural attributes. Therefore, careful consideration of these issues should be taken when applying the method developed in this study to other cities or at different seasons in addition to recalibrating satellite images. More research on relationships between vegetation indices and urban vegetation structural attributes for different seasons and cities should be considered in the future.

5 Conclusion

Based on multitemporal Landsat TM data (1997, 2004 and 2010) and urban vegetation field survey data, this study explored the potential of using TM imagery in estimating urban vegetation structural attributes and analyzed spatiotemporal dynamics of urban vegetation structural attributes in the city of Changchun, China. The following conclusions could be drawn:

1) NDVI is a good predictor of some urban vegetation structural attributes for building urban vegetation structural estimation models to estimate and map urban vegetation structural attributes.
2) Some urban vegetation structural attributes (e.g., crown closure (CC), basal area (BA), and leaf area index (LAI)) could be retrieved and estimated by NDVI index but some could not (e.g., stem density, diameter at breast height, and tree height). The result shows that urban vegetation is structurally different from natural vegetation.
3) In the well-urbanized region of Changchun City, the urban vegetation structure was found to change significantly from 1997 to 2004 and from 2004 to 2010. Urban vegetation structural attributes: CC, LAI, and BA in the study area decreased sharply from 1997 to 2004 and slightly increased from 2004 to 2010. The increase in urban vegetation in Changchun from 2004 to 2010 may be due to the improvement of urban vegetation quality and quantity associated with growth of vegetation. The CC, LAI, and BA class distributions were all skewed toward low values in 1997 and 2004, but they were skewed toward relatively high values in 2010.
4) The experimental results demonstrate that Landsat TM imagery could provide a fast and cost-effective method to obtain a spatiotemporal 30-m resolution urban vegetation structural dataset (including CC, LAI, and BA).

This method developed in this study should be a useful application of Landsat TM data in various urban vegetation management practices, and the results created from this study provide necessary baseline information in terms of relatively high-resolution urban vegetation structural attribute maps. Furthermore, the accurate information of urban vegetation structural attributes may provide urban planners with more accurate data and allow better planting designs for urban vegetation at a landscape level.

Acknowledgements This research was supported by The CAS/SAFEA International Partnership Program for Creative Research Teams (KZZD-EW-TZ-07-09), Foundation for Excellent Young Scholars of Northeast Institute of Geography and Agroecology, Chinese Academy of Sciences (DLSYQ13004), and One Hundred Talents Program in Chinese Academy of Sciences (Grand No. Y3H1051001). The authors also want to provide our great gratitude to the editors and the anonymous reviewers who gave us their insightful comments and suggestions.

References

Armson D, Stringer P, Ennos AR (2013) The effect of street trees and amenity grass on urban surface water runoff in Manchester, UK. Urban For Urban Green 12:282–286. doi:10.1016/j.ufug.2013.04.001

Baret F, Guyot G (1991) Potentials and limits of vegetation indexes for LAI and APAR assessment. Remote Sens Environ 35:161–173. doi:10.1016/0034-4257(91)90009-U

Bowler DE, Buyung-Ali L, Knight TM, Pullin AS (2010) Urban greening to cool towns and cities: a systematic review of the empirical evidence. Landsc Urban Plan 97:147–155. doi:10.1016/j.landurbplan.2010.05.006

Cao S, Chen L, Liu Z (2009) An investigation of Chinese attitudes towards the environment: case study using the Grain for Green Project. Ambio 38:55–64. doi:10.1579/0044-7447-38.1.55

Chander G, Markham B (2003) Revised Landsat-5 TM radiometric calibration procedures and post calibration dynamic ranges. IEEE T Geosci Remote Sens 41:2674–2677. doi:10.1109/TGRS.2003.818464

Clark DA, Brown S, Kicklighter DW, Chambers JQ, Thomlinson JR (2001) Measuring net primary production in forests: concepts and field methods. Ecol Appl 11(2):356–370. doi:10.1890/1051-0761(2001)011

Cohen WB, Spies TA, Fiorella M (1995) Estimating the age and structure of forests in a multi-ownership landscape of western Oregon, USA. Int J Remote Sens 16:721–746. doi:10.1080/01431169508954436

Convertino M, Muñoz-Carpena R, Chu-Agor ML, Kiker GA, Linkov I (2014) Untangling drivers of species distributions: global sensitivity and uncertainty analyses of MAXENT. Environ Model Softw 51:296–309. doi:10.1016/j.envsoft.2013.10.001

Cornelis J, Hermy M (2004) Biodiversity relationships in urban and suburban parks in Flanders. Landsc Urban Plan 69:385–401. doi:10.1016/j.landurbplan.2003.10.038

Du P, Li X, Cao W, Luo Y, Zhang H (2010) Monitoring urban land cover and vegetation change by multi-temporal remote sensing information. Min Sci Tech 20(6):922–932. doi:10.1016/S1674-5264(09)60308-2

Dwivedi P, Rathore SC, Dubey Y (2009) Ecological benefits of urban forestry: the case of Kerwa Forest Area (KFA), Bhopal, India. Appl Geogr 29:194–200. doi:10.1016/j.apgeog.2008.08.008

Figueiredo EO, Neves d'Oliveira MV, Braz EM (2016) LIDAR-based estimation of bole biomass for precision management of an Amazonian forest: comparisons of ground-based and remotely sensed estimates. Remote Sens Environ 187:281–293. doi:10.1016/j.rse.2016.10.026

Fowler D, Skiba U, Nemitz E, Choubedar F, Branford D (2004) Measuring aerosol and heavy metal deposition on urban woodland and grass using inventories of 210Pb and metal concentrations in soil. Water Air Soil Pollut 4:483–499. doi:10.1023/B:WAFO.0000028373.02470

Franklin SE, Giles PT (1995) Radiometric processing of aerial and satellite remote sensing imagery. Comput Geosci 21:413–425. doi:10.1016/0098-3004(94)00085-9

Franklin J, Hiernaux PHY (1991) Estimating foliage and woody biomass in Sahelian and Sudanian woodlands using a remote sensing model. Int J Remote Sens 12(6):1387–1404. doi:10.1080/01431169108929732

Freitas SR, Mello MCS, Cruz CBM (2005) Relationships between forest structure and vegetation indices in Atlantic rainforest. For Ecol Manag 218:353–362. doi:10.1016/j.foreco.2005.08.036

Frolking S, Palace M, Clark DB, Chambers JQ, Shugart HH, Hurtt GC (2009) Forest disturbance and recovery—a general review in the context of space-borne remote sensing of impacts on aboveground biomass and canopy structure. J Geophys Res 114:G00E02. doi:10.1029/2008JG000911

Godefroid S, Koedam N (2003) How important are large vs. small forest remnants for the conservation of the woodland flora in an urban context. Glob Ecol Biogeogr 12:287–298. doi:10.1046/j.1466-822X.2003.00035.x

Gower ST, Kucharik CJ, Norman JM (1999) Direct and indirect estimation of leaf area index, fAPAR, and net primary production of terrestrial ecosystems. Remote Sens Environ 70:29–51. doi:10.1016/S0034-4257(99)00056-5

Gray J, Song C (2012) Mapping leaf area index using spatial, spectral, and temporal information from multiple sensors. Remote Sens Environ 119:173–183. doi:10.1016/j.rse.2011.12.016

Guo Z, Wang Z, Song K, Zhang B, Li F, Liu D (2007) Correlations between forest vegetation NDVI and water/thermal condition in Northeast China forest regions in 1982–2003. Chin J Ecol 26(12):1930–1936 (In chinese)

Hall RJ, Skakun RS, Arsenault EJ, Case BS (2006) Modeling forest stand structure attributes using Landsat ETM+ data: application to mapping of aboveground biomass and stand volume. For Ecol Manag 225:378–390. doi:10.1016/j.foreco.2006.01.014

Harold SJZ, Janet LO, Heather MR (2014) Influence of lidar, Landsat imagery, disturbance history, plot location accuracy, and plot size on accuracy of imputation maps of forest composition and structure. Remote Sens Environ 143:26–38. doi:10.1016/j.rse.2013.12.013

Huang X, Huang XJ, Chen C (2009) The characteristic, mechanism and regulation of urban spatial expansion of Changchun. Areal Res Dev 5:68–72 (In chinese)

Hutyra LR, Yoon B, Alberti M (2010) Terrestrial carbon stocks across a gradient of urbanization: a study of the Seattle, WA region. Glob Chang Biol 17:783–797. doi:10.1111/j.1365-2486.2010.02238.x

Ingram JC, Terence P, Dawson J, Whittaker (2005) Mapping tropical forest structure in southeastern Madagascar using remote sensing and artificial neural networks. Remote Sens Environ 94:491–507. doi:10.1016/j.rse.2004.12.001

Ji L, Wylie BK, Nossov DR, Peterson B, Waldrop MP, McFarl JW, Rover J, Hollingsworth TN (2012) Estimating aboveground biomass in interior Alaska with Landsat data and field measurements. Int J Appl Earth Obs 18:451–461. doi:10.1016/j.jag.2012.03.019

Kayitakire F, Hamel C, Defourny P (2006) Retrieving forest structure variables based on image texture analysis and IKONOS-2 imagery. Remote Sens Environ 102:390–401. doi:10.1016/j.rse.2006.02.022

Kirnbauer MC, Baetz BW, Kenney WA (2013) Estimating the stormwater attenuation benefits derived from planting four monoculture species of deciduous trees on vacant and underutilized urban land parcels. Urban For Urban Green 12:401–407. doi:10.1016/j.ufug.2013.03.003

Kong F, Nakagoshi N (2006) Spatial-temporal gradient analysis of urban green spaces in Jinan, China. Landsc Urban Plan 78:147–164. doi:10.1016/j.landurbplan.2005.07.006

Landry SM, Chakraborty J (2009) Street trees and equity: evaluation the spatial distribution of an urban amenity. Environ Plan 41:2651–2670

LaPaixa R, Freedmanc B (2010) Vegetation structure and composition within urban parks of Halifax Regional Municipality, Nova Scotia, Canada. Landsc Urban Plan 98:124–135. doi:10.1016/j.landurbplan.2010.07.019

Lefsky MA, Cohen WB, Acker SA, Parker GG, Spies TA, Harding DJ (1999) Lidar remote sensing of the canopy structure and biophysical properties of Douglas-fir western hemlock forests. Remote Sens Environ 70:339–361. doi:10.1016/S0034-4257(99)00052-8

Li X, Zhou W, Ouyang Z (2013) Relationship between land surface temperature and spatial pattern of greenspace: what are the effects of spatial resolution. Landsc Urban Plan 114:1–8. doi:10.1016/j.landurbplan.2013.02.005

Lu D, Paul M, Eduardo B, Emilio M (2004) Relationships between forest stand parameters and Landsat TM spectral responses in the Brazilian Amazon Basin. For Ecol Manag 198:149–167. doi:10.1016/j.foreco.2004.03.048

Marc L, Ping Z, Robert EW, Lahouari B (2010) Remote sensing of the urban heat island effect across biomes in the continental USA. Remote Sens Environ 114:504–513. doi:10.1016/j.rse.2009.10.008

Martin S, Doris K, Christopher C, Stefan D, Heiko P (2014) On the relationship between vegetation and climate in tropical and northern Africa. Theor Appl Climatol 115:341–353. doi:10.1007/s00704-013-0900-6

McPherson EG, Simpson JR (1998) Air pollutant uptake by Sacramento's urban forest. J Arboricult 24:224–234

Mcpherson EG, Nowak D, Gordon H (1997) Quantifying urban forest structure, function, and value: the Chicago Urban Forest Climate Project. Urban Ecosyst 1:49–61

McPherson EG, Simpson JR, Peper PJ, Maco SE, Xiao Q (2005) Municipal forest benefits and costs in five U.S. cities. J Forest 103:411–416

Miller MD (2012) The impacts of Atlanta's urban sprawl on forest cover and fragmentation. Appl Geogr 34:171–179. doi:10.1016/j.apgeog.2011.11.010

Miller PR, Winer AM (1984) Composition and dominance in Los Angeles basin urban vegetation. Urban Ecol 8:29–54. doi:10.1016/0304-4009(84)90005-6

Myeong S, Nowak DJ, Duggin MJ (2006) A temporal analysis of urban forest carbon storage using remote sensing. Remote Sens Environ 101:277–282. doi:10.1016/j.rse.2005.12.001

Naesset E, Okland T (2002) Estimating tree height and tree crown properties using airborne scanning laser in a boreal nature reserve. Remote Sens Environ 79:105–115. doi:10.1016/S0034-4257(01)00243-7

Nowak DJ (1994) Understanding the structure of urban forests. J Forest 92:36–41

Nowak DJ, Crane DE (2002) Carbon storage and sequestration by urban trees in the USA. Environ Pollut 116:381–389. doi:10.1016/S0269-7491(01)00214-7

Nowak DJ, Crane DE, Stevens JC, Hoehn RE (2003) The Urban Forest Effects (UFORE) model: field data collection manual. US Department of Agriculture Forest Service, Northeastern Research Station, Syracuse, NY

Nowak DJ, Crane DE, Stevens JC (2006) Air pollution removal by urban trees and shrubs in the United States. Urban For Urban Green 4(3–4):115–123. doi:10.1016/j.ufug.2006.01.007

Piao S, Fang J, Zhou L, Guo Q, Mark H, Ji W (2003) Interannual variations of monthly and seasonal normalized difference vegetation index (NDVI) in China from 1982 to 1999. J Geophys Res Atmos 108:1–13. doi:10.1029/2002JD002848

Pu R, Gong P (2004) Wavelet transform applied to EO-1 hyperspectral data for forest LAI and crown closure mapping. Remote Sens Environ 91:212–224. doi:10.1016/j.rse.2004.03.006

Ren Z, He X, Zheng H, Zhang D, Yu X, Shen G, Guo R (2013) Estimation of the relationship between urban park characteristics and park cool island intensity by remote sensing data and field measurement. Forests 4:868–886. doi:10.3390/f4040868

Rogan J, Millerr J, Stow D, Franklin J, Levien L, Fischer C (2003) Land-cover change monitoring with classification trees using Landsat TM and ancillary data. Photogramm Eng Rem S 69(7):793–804. doi:10.14358/PERS.69.7.793

Roy PS, Ranganath BK, Diwakar PG, Vohra TPS, Bhan SK, Singh IJ, Pandian VC (1991) Tropical forest type mapping and monitoring using remote sensing. Int J Remote Sens 12:2205–2225. doi:10.1080/01431169108955253

Schneider A (2012) Monitoring land cover change in urban and peri-urban areas using dense time stacksof Landsat satellite data and a data mining approach. Remote Sens Environ 124:689–704. doi:10.1016/j.rse.2012.06.006

Seto KC, Woodcock CE, Song C, Huang X, Lu J, Kaufmann RK (2002) Monitoring land-use change in the Pearl River Delta using LandsatTM. Int J Remote Sens 23:1985–2004. doi:10.1080/01431160110075532

Shashua-Bar L, Hoffman ME (2000) Vegetation as climatic component in the design of an urban street—an empirical model for predicting the cooling effect of urban green areas with trees. Energy Build 31:221–235. doi:10.1016/S0378-7788(99)00018-3

Tooke TR, Klinkenberg B, Coops NC (2010) A geographical approach to identifying vegetation-related environmental equity in Canadian cities. Environ Plan 37:1040–1056. doi:10.1068/b36044

Townshend JRG, Justice CO (1986) Analysis of the dynamics of African vegetation using the normalized difference vegetation index. Int J Remote Sens 7(11):1435–1445. doi:10.1080/01431168608948946

Trammell TLE,CarreiroMM (2011) Vegetation composition and structure of woody plant communities along urban interstate corridors in Louisville, KY, USA. Urban Ecosyst 14:501–524. Doi: 10.1007/s11252-011-0193-4

Turner DP, Cohen WB, Kennedy RE, Fassnacht KS, Briggs JM (1999) Relationships between leaf area index and Landsat TM spectral vegetation indices across three temperate zone sites. Remote Sens Environ 70:52–68. doi:10.1016/S0034-4257(99)00057-7

Weishampel JF, Blair JB, Knox RG, Dubayah R, Clark DB (2000) Volumetric lidar return patterns from an old-growth tropical rainforest canopy. Int J Remote Sens 21:409–415. doi:10.1080/014311600210939

Xiao QF, McPherson EG, Ustin SL, Grismer ME, Simpson JR (2000) Winter rainfall interception by two mature open-grown trees in Davis, California. Hydrol Process 14:763–784

Yang X, Lo CP (2000) Relative radiometric normalization performance for change detection from multi-date satellite images. Photogram Eng Rem S 66(8): 967–980. Doi: 2-s2.0–0033873756

Young RF (2010) Managing municipal green space for ecosystem services. Urban For Urban Green 9:313–321. doi:10.1016/j.ufug.2010.06.007

Zhang D, Zheng H, Ren Z, Zhai C, Shen G, Mao Z, Wang P, He X (2015) Effects of Forest type and urbanization on carbon storage of UrbanForests in Changchun. Northeast China Chin Geogr Sci 25:147–158. doi:10.1007/s11769-015-0743-4

Zhou X, Wang Y (2011) Spatial–temporal dynamics of urban greenspace in response to rapid urbanization and greening policies. Landsc Urban Plan 100: 268–277. Doi: 10.1016/j.landurbplan.2010.12.013